JOURNAL OF CATALYSIS 157, 645–655 (1995)

Ethyl *tert*-Butyl Ether (ETBE) Synthesis on H–Mordenite: Gas-phase Kinetics and DRIFTS Studies

Gustavo Larsen,[1] Edgar Lotero, Manuel Márquez, and Hugo Silva

Department of Chemical Engineering, University of Nebraska-Lincoln, Lincoln, Nebraska 68588-0126

Received March 28, 1995; revised August 18, 1995; accepted August 21, 1995

The ethyl *tert*-butyl ether (ETBE) formation between 313 and 363 K over an H–mordenite catalyst was studied in a packed-bed flow catalytic reactor at atmospheric pressure. An activation energy of 82 kJ/mol and reaction orders in isobutene and ethanol of 0.8 and −0.8 were found. *In situ* diffuse reflectance Fourier transform infrared spectroscopy (DRIFTS) was used to study the state of the catalyst under reaction conditions. The IR studies, coupled with the reaction kinetics information, are consistent with the idea that the stability of the H–mordenite catalyst requires the protective action of ethanol to prevent the occurrence of isobutene oligomerization products. The high ethanol concentrations found in the zeolite pores under the temperature and pressure conditions employed is also responsible for reaction inhibition.

1. INTRODUCTION

Recently, effort has been made to understand the synthesis of methyl *tert*-butyl ether (MTBE) and ethyl *tert*-butyl ether (ETBE) over solid acid catalysts, due to the importance of such oxygenates as environmentally sound gasoline additives (1–9). In particular, ETBE can be obtained catalytically by reacting isobutene with ethanol, the latter being a renewable energy resource. While the issue of meeting the oxygen content standards in gasolines by using either ETBE or MTBE remains controversial (10), the processes leading to these two oxygenates are very similar (5, 11), suggesting that MTBE plants could be adapted for ETBE production and vice versa. The synthesis of ETBE or MTBE involves liquid–solid heterogeneous kinetics and makes use of sulfonic resins as acid catalysts, such as the Amberlyst-15. The commercial process requires the use of low isobutene/alcohol ratios which constitutes a practical disadvantage given the fact that the excess alcohol has to be recycled. Thus, zeolite-based catalysts appear to be a promising alternative (12).

The formation of MTBE over sulfonic resins increases more than linearly with the number of $-SO_3H$ groups in the catalyst (11). For resin-catalyzed alcohol dehydrations, Thornton and Gates (13) proposed that the reaction requires the participation of more than one acid site, a concept that may well be extended to the reactions of isobutene with methanol or ethanol (6). The ionic (carbenium ion) mechanism is supported by the fact that, when using isoamylenes instead of isobutene, the double bond shift of the alkene always accompanies the formation of the ether (11). In addition, longer chain alcohols undergo etherification at higher rates (11). Given the inhibitor character of the alcohol at low alcohol/isobutene ratios, and the zero-order dependence of the reaction rate with alcohol concentration at alochol/isobutene ratios close or above stoichiometric, it is believed that the alcohol-coordinated proton is responsible for a transition from a concerted mechanism to an ionic one, the latter taking place at a substantially lower reaction rate. Unfortunately, this same level of mechanistic understanding has not yet been achieved for the zeolite-catalyzed reaction. Several authors have proposed the use of acidic zeolites for MTBE and ETBE synthesis (3, 7–9). While some researchers favor the idea that it is the olefin that interacts with the acid site first (9), others have proposed that it is a hydrogen-bonded or even a protonated alcohol, acting as the electrophilic species, that reacts with the olefin double bond (3). Taking into account Lowenstein's rule, the mechanism of ETBE (or MTBE) formation on zeolites is likely to differ from that proposed for sulfonic resins, if we accept the idea that the latter requires that more than one $-SO_3H$ group be involved in the reaction at the same time.

Zeolites typically display lower specific activities than the Amberlyst-15 catalyst (3). This may be perhaps the major obstacle to overcome for practical applications. Nevertheless, their pore structure can impose restrictions on the formation of undesirable by-products, especially those that originate from bulky intermediates. For example, the bimolecular isobutene oligomerization reaction pathway could in principle be suppressed by the narrow, unidirectional channels of certain zeolites. Zeolite H-ZSM-5 has

[1] To whom all correspondence should be addressed.

0021-9517/95 $12.00

been proposed by Tau and Davis (9) for ETBE synthesis, even though the molecular critical size (MCS) of ETBE and MTBE (approximately 0.62 nm) exceeds the pore mouth of H-ZSM-5 by about 0.1 nm. Although a molecule such as 2,2-dimethylbutane, which has essentially the same MCS as ETBE or MTBE, is capable of diffusing into the H-ZSM-5 pores, such configurational intracrystalline transport displays an activation energy (14) comparable to those normally found in literature for ETBE and MTBE production under kinetically-controlled regimes (8). Thus, we have chosen H–mordenite due to its large pore diameter (0.67 × 0.70 nm), essentially unidirectional channel structure, and high acid strength.

The objective of this work is to shed some light on the nature of ETBE formation on H–mordenite at low conversions. When carrying out gas-phase kinetics with zeolites and alcohols as reactants (14, 15), the extent of pore-filling is high and results may still be of some relevance to liquid-phase kinetics.

2. EXPERIMENTAL

2.1. Materials

The mordenite sodium form was kindly donated by Dr. Alan Risch from UOP, Tarrytown, NY. It has a Si/Al ratio of 6.4. The H–mordenite catalyst was obtained by carrying out the following sequence twice. The Na cations were ion-exchanged at room temperature with NH_4^+ using a 0.5 *N* solution of ammonium nitrate (Aldrich). A suspension of 5 g of Na-Mordenite in 0.5 liter of the NH_4^+ solution was stirred for 48 h. The solids were filtered and washed with distilled water, dried overnight at 408 K, and subsequently calcined at 873 K for 1 h to produce the hydrogen form by destruction of NH_4^+ ions. Absolute ethanol (99.5+%, McCormick Distilling Co.), research grade isobutene (99.75% minimum purity), and ultra-high purity air (Matheson) were used without further purification. Ultra-high purity nitrogen was further purified using commercial oxygen and water traps. The chemical analysis of samples was done at Galbraith Laboratories.

2.2. Kinetic Studies

A conventional atmospheric, gas-phase stainless-steel flow reaction system equipped with Brooks 5850 mass-flow controllers was used for the kinetic runs. Gas chromatographic (GC) quantification of products was carried out with a Hewlett-Packard 5880 GC, a 80/120 Carbopak B column from Supelco and calibrated flame ionization detection of each species exiting the reactor. The catalyst bed (typically 50–100 mg) was placed in a 4-mm i.d. Pyrex U-tube with an α-Al_2O_3 (1–2 m^2/g) packing as a preheating bed. The H–mordenite was pelletized, crushed, and sieved to collect the 20–40 mesh fraction. The temperature was controlled externally to ±0.5 K.

The desired ethanol partial pressure was achieved by bubbling nitrogen at a chosen flow rate through a saturator kept at 283 K by means of a recirculating chiller. To obtain the ethanol and isobutene reaction orders and compensate for the variable partial pressure (flow rate), a third mass-flow controlled steam (nitrogen) was introduced. Total flow rates of 51 cc/min were used. Conversion levels were kept below 1–2%. Reaction rates are reported per gram of catalyst. The high activation energy found, which is in agreement with previously reported data, coupled with the fact that the largest product molecules have an MCS *smaller* than the H–mordenite pore diameter (16) suggest that intraparticle and intracrystalline diffusion limitations are not likely to be important. Prior to reaction, the H–mordenite sample was reactivated under an air flow at 723 K for 1 h and subsequently purged with nitrogen until the desired reaction temperature was stabilized. The reactor was by-passed and all flow rates were set to their chosen values prior to admitting reactants into the reactor. No detectable amounts of diethyl ether (a common by-product in the integral reactor) were found. Apart from ETBE, isobutene dimers and heavier products were only detected in the product stream when the alcohol flow was interrupted. Flow-switching experiments in which one of the reactants is replaced with pure N_2 were conducted, as well as adsorption experiments to estimate the amount of isobutene and alcohol admitted in the zeolite pores prior to achieving a steady state.

2.3. DRIFTS Measurements

In situ DRIFTS studies were carried out at 337 K on a Nicolet 20 SXB Fourier transform infrared spectrometer equipped with a commercial DRIFTS catalytic chamber and associated optical and temperature control systems from Spectratech. The reactor part of the cell consists of a temperature-controlled ceramic cup where the catalyst powder is packed and reactants are allowed to flow through. A similar stainless steel reaction system to that described in Section 2.2. was used, except for the incorporation of a conventional GC 8-port valve before the reactor inlet that allows for pulse injection and switching of reactants. Typically, 0.05 g of H–mordenite were placed in the DRIFTS cell and pretreated as indicated in Section 2.2. Spectra were collected every minute for about 0.5 min in the wavenumber interval 4000–400 cm^{-1} (resolution 4 cm^{-1}) for transient work. For steady-state experiments 100 scans (total acquisition time, 10 min) were collected. Spectra are presented after the Fourier-transformed data in a reflectance scale has been converted to Kubelka–Munk units.

TABLE 1

Catalyst Properties

Sample	BET surface area (m^2/g)	Na wt%	EtOH Uptake[a] (mmol/g)	isobutene Uptake[a] (mmol/g)
Na-mordenite	178	3.66	—	—
H-mordenite	183	0.05	2.3	0.3

[a] The uptakes were calculated by sorption transients and cofeeding at a ethanol/isobutene ratio of 0.55. P_{isob} = 0.7 kPa, balance: N_2 to 101.3 kPa.

3. RESULTS AND DISCUSSION

The catalyst and catalyst precursor chemical compositions and dynamic adsorption capacities are shown in Table 1. Chemical analysis reveals that essentially all Na^+ ions are removed from the lattice by the sequential ion-exchange process, but the BET sorption properties of the starting material are not modified significantly. The extent of ion-exchange indicates that roughly 1.6 mmol H^+/g had been created, assuming the Na wt% difference between the Na-mordenite precursor and the calcined catalyst is compensated by an equal amount (on a mol basis) of lattice protons. It should be mentioned that surface area measurements may be obscured by capillary condensation in narrow pore materials, but the purpose of the BET measurements here is to draw a qualitative comparison between the two materials before and after the ion-exchange/calcination step. X-ray diffraction (Rigaku DMAX/IIB diffractometer with Cu$K\alpha$ radiation) confirmed the integrity of the mordenite lattice after the ammonolysis step.

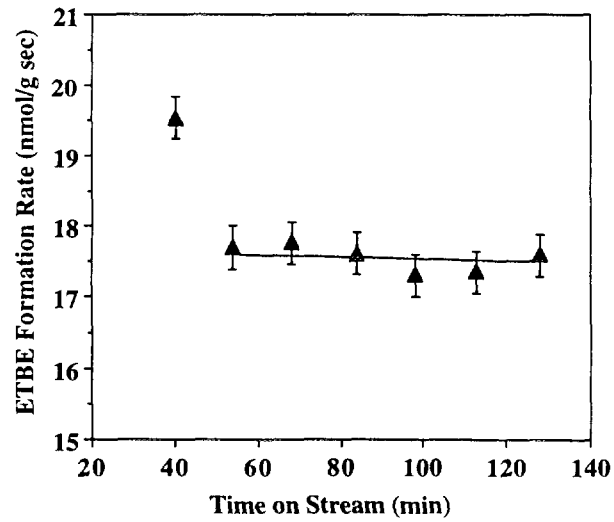

FIG. 2. Rate of ETBE formation vs time on stream. P_{isob} = 0.70 kPa; ethanol/isobutene ratio, 0.96; Balance, N_2 to 101.3 kPa; T = 337 K.

3.1. Reaction Studies

Figure 1 shows the dependence of the ETBE formation rate with the reactant partial pressure at 329 K. Reaction orders in isobutene and ethanol were found to be 0.8 and −0.8, respectively. The activation energy was found to be 82 kJ/mol in the range 337–313 K. This value compares well with previously reported activation energies for ETBE (8) and MTBE (3) formation. A typical time on stream vs reaction rate curve is shown in Fig. 2. During a cofeeding startup, the catalyst was found to reach a very stable activity plateau after an initial deactivation period. The reaction

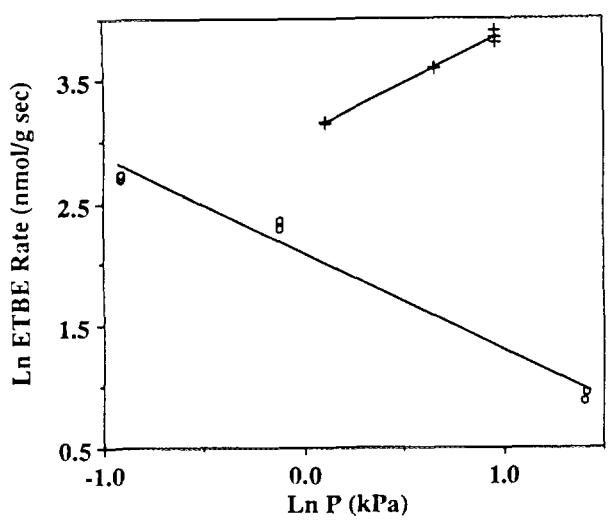

FIG. 1. ln ETBE formation rate vs. ln reactant partial pressure. (+) for isobutene, with P_{EtOH} = 0.3 kPa, (○) for ethanol, with P_{isob} = 0.7 kPa.

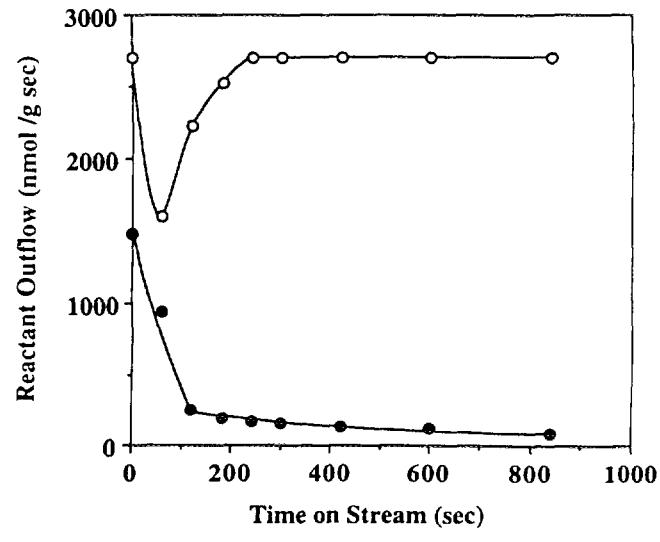

FIG. 3. Effect of replacing the ethanol flow with nitrogen on the reactant outflow composition. (●) ethanol, (○) isobutene.

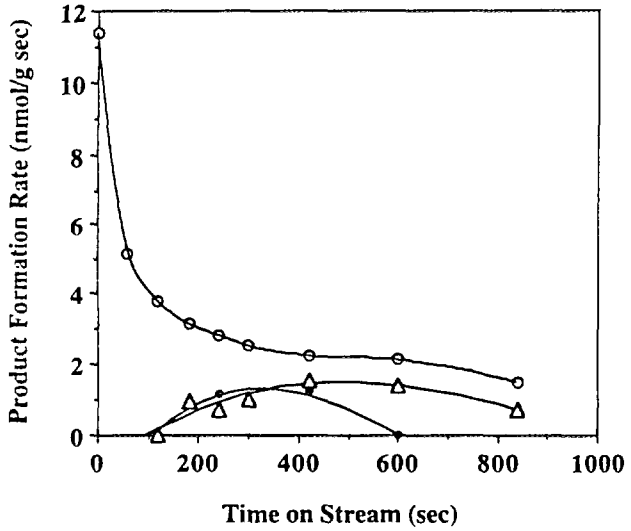

FIG. 4. Product distribution after interruption of the ethanol flow. (○) ETBE, (△) diisobutene, (●) heavier products.

orders and activation energy were derived from this activity plateau. Within the experimental error resulting from setting up a new catalyst bed (10–15%), the catalyst showed no isotopic effect when using EtOD. Figures 3 and 4 show the effect of replacing the alcohol flow with N_2 using a four-way valve in the reactor manifold. The removal of about 0.156 mmol/g ethanol at 329 K is accompanied by the incorporation of an additional 0.10 mmol/g isobutene (Fig. 3), and oligomerization products start being detected (see Fig. 4). The replacement of the isobutene flow with N_2 only gave a monotonic decrease in ETBE production (only product detected). Adsorption experiments and corrections for reactor manifold dead space allowed us to estimate the uptake data shown in Table 1. Product formation played a negligible role in calculating the uptakes in Table 1 since the amount of product detected was always less than 2% during the adsorption of reactants. As a reference point, the room-temperature isobutane uptake of H–mordenite at 50 torr is approximately 0.69 mmol/g (18), which suggests that under the reaction conditions employed here, the zeolite pores have a high reactant concentration. In the absence of isobutene in the feed, an additional 0.3 mmol/g ethanol are adsorbed by the zeolite indicatng that, during the cofeeding startup of the reactor, part of the zeolite volume is filled with either isobutene or oligomerization products. This is an important aspect since we are aware of the possibility that the uptake values in Table 1 may not reflect the true uptake of isobutene and ethanol under a steady state because the formation of small amounts of heavy products during startup might have led us to overestimate these values. Nevertheless, from Table 1 and Fig. 3, it is apparent that a substantial amount of ethanol originally allowed in the reactor is removed by neither N_2 purging nor N_2 reaction. However, when the small, reversible alcohol pore concentration is depleted, it appears that isobutene oligomerization starts taking place at detectable rates.

Figure 5 shows the ETBE/reactant ratios during flow-switching experiments. The denominator in these ratios is given by the gas-phase concentration of the reactant species (either isobutene or ethanol) being replaced with an equal flow of pure nitrogen. The figure shows that a depletion of gas-phase isobutene during a flow-switching experiment essentially matches a decrease in the ETBE production rate, resulting in a constant gas-phase ETBE/isobutene ratio in the reactor outflow. This is in agreement with the nearly first-order dependence of the reaction on isobutene (see Fig. 1). On the other hand, the decrease in ETBE formation is delayed with respect to the disappearance of gas-phase ethanol as shown by the ETBE/ethanol ratio in Fig. 5. *A priori*, we expected in this case an absolute increase in the ETBE formation rate given the negative reaction order in ethanol, but this was not observed (see Fig. 4). This may be due to the fact that reaction orders are derived from steady-state measurements, in which the behavior of adsorbed species may differ from that observed during nonsteady-state situations. In order to provide a tentative explanation for the absence of an absolute increase in the ETBE formation rate during alcohol desorption solely based on limited kinetic information presented thus far, we have to consider at least two different scenarios. The purpose of the DRIFTS experiments shown below is to strengthen and complement some of these ideas. (i) If the olefin reacts with preadsorbed alcohol as recently

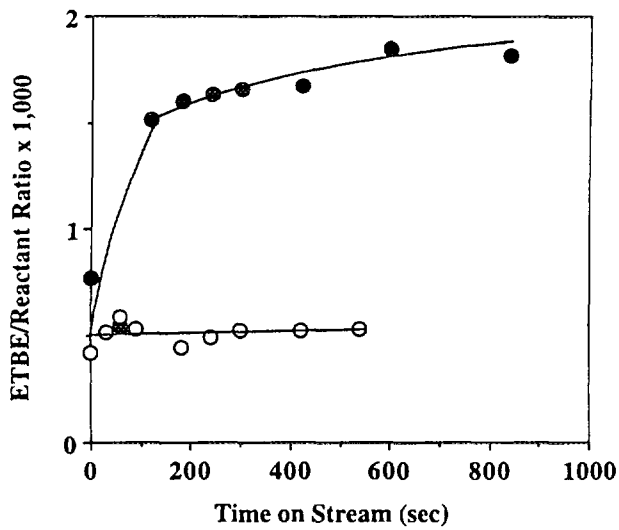

FIG. 5. Gas-phase ETBE/reactant ratios during replacement of one of the reactants' flow with an equal flow of nitrogen. ETBE/isobutene ratio during gas-phase isobutene removal (○) and ETBE/ethanol ratio during ethanol removal (●).

suggested (16), then one would expect the possibility of clustering of alcohol molecules, as recently proposed by Mirth *et al.* (19), to account for the negative reaction order in ethanol. Note that hydrogen-bonded alcohol dimers and trimers interacting with the acid site would not only result in a steric hindrance for the approaching olefin molecule, but also in a less effective electrophilic species to attack the double bond due to charge dissipation. A higher degree of clustering at higher pressures would explain the inhibitory effect of ethanol. On the other hand, it is still possible that during the abrupt perturbation of the steady state by means of ethanol–N_2 switching, a few acid sites are abandoned without declustering, causing acid sites to be lost for ETBE production (and not gained by decomposition of the cluster first) but making them available for isobutene oligomerization. Haase and Sauer (20) carried out theoretical calculations to estimate the ^{1}H NMR chemical shifts of methanol in zeolites. These authors also optimized the structure of two methanol molecules interacting with a single zeolite acid site, in an attempt to explain the previously observed ^{1}H NMR chemical shifts (19). Given the ethanol uptake in Table 1, the estimated acid site density (1.6 mmol H^+/g), and the sterically restricted zeolite environment, we do not expect such clusters to be composed of more than two or three ethanol molecules. The idea that such very small alcohol clusters could abandon the acid site without separating into individual ethanol molecules remains to be tested by theory. However, this picture could explain both the negative reaction order in ethanol and the absence of an absolute maximum in the ETBE production rate upon interruption of the ethanol feed. (ii) The second possibility is that the olefin interacts with the acid site first (9). In this case, a high alcohol pore occupancy and/or the blocking of acid sites by ethanol would be responsible for its negative reaction order. Again, if during ethanol desorption the zeolite pores are deprived from single ethanol molecules and ethanol–H^+ interactions faster than the rate of alcohol cluster decomposition then the ETBE formation rate may well not increase as the overall concentration of alcohol in the pore drops because fast oligomerization may quickly take over. The rate of olefin oligomerization over acidic zeolites increases markedly with double bond substitution (21).

During ethanol feed interruption the data in Fig. 4 are also consistent with the idea of a retreating shell of liquid ethanol with ETBE produced at the shell boundary. We have chosen to picture this process microscopically given the small size of the zeolite cavities. Nevertheless, the equivalence of these two models is given by the fact that the gradual disappearance of small alcohol clusters can be taken as the retreating liquid shell in the more macroscopic picture.

At this point, the observation that only a small fraction of alcohol was desorbed during flow switching experiments could either imply that (i) ethanol molecules remained strongly bonded to the zeolite or that (ii) ethanol formed heavier products (heavier ethers) during the cofeeding startup. A temperature-programmed desorption experiment of preadsorbed alcohol proved to be inconclusive since we observed that only less than 10% of the ethanol desorbs, accompanied by the evolution of trace amounts of ethene and the deep-browning of the catalyst bed, suggesting that coking had taken place.

Given the several different possibilities, we decided to divert our attention to performing *in situ* DRIFTS experiments in the same temperature and pressure range. The DRIFTS cell also operated as a once-through packed-bed reactor and allowed us to conduct a series of experiments by systematically varying the feed composition while monitoring the adsorbed species during the reaction.

3.2. *DRIFTS Experiments*

Figure 6 shows the evolution of the hydroxyl and C–H stretching regions with pulse addition of ethanol at low dosages. Alcohol addition initially causes broadening of

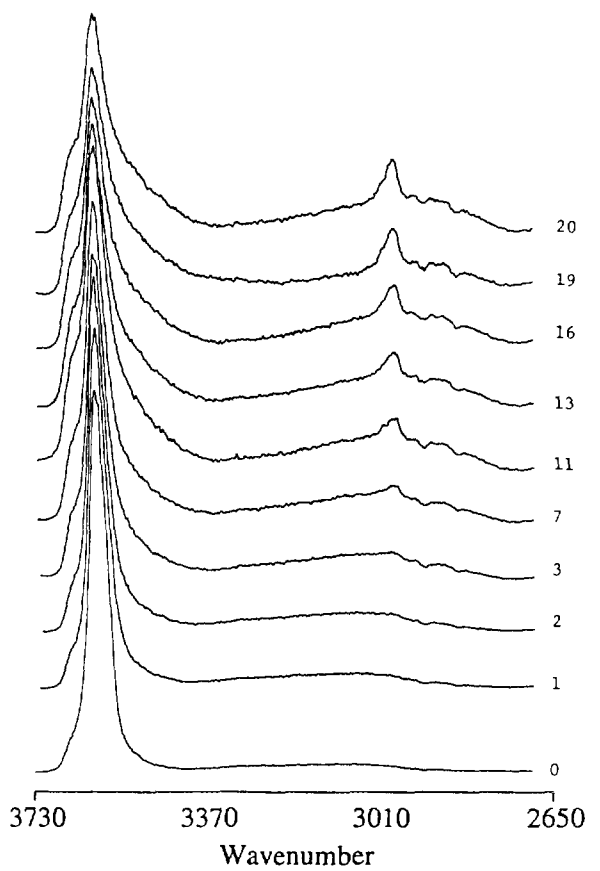

FIG. 6. Effect of pulse addition of gas-phase ethanol to H–mordenite. Pulse size: 1 μmol (1.25×10^{-2} mol ethanol/mol H^+). The number of pulses is specified in each case. Full scale: 0.32 Kubelka–Munk units.

the high frequency OH- region and appearance of new C–H stretching and O–H deformation bands around 2850–3000 cm^{-1}. It should be pointed out that the latter may also be a convolution of those two bands with the downward shifted zeolite O–H stretching. No O–H stretching band higher than 3700 cm^{-1} was observed. Interestingly, upon ethanol saturation the sharp zeolite O–H stretching signal disappears, and the broadening observed at low alcohol loadings is also accompanied by a red shift (see Fig. 7). It seems that that it is only at alcohol coverages above 1 (with respect to the calculated acid site density in Table 1) that the O–H frequency decreases considerably. The fact that excess alcohol causes this shift is consistent with the idea that more than one adsorbate molecule may cluster around the acid site. The O–H stretching of alcohols is typically found in the range 3500–3600 cm^{-1}. Figures 6 and 7 both show the presence of strong hydrogen bonding, given the pronounced line broadening upon alcohol loading. Using ^1H NMR and FTIR to study the methanol/H-ZSM5 system, Mirth *et al.* (19) suggested that a broad O–H stretching band around 3300 cm^{-1} was due to the formation of short hydrogen-bridged alcohol chains, and that the chains may interact with different zeolite O–H groups due to rapid rotation. These authors suggested that the magnitude of the red shift was proportional to the methanol chain length. In our case, we did not observe such a band during continuous alcohol feed regardless of the isobutene partial pressure. The shift in the O–H stretching frequency is rather modest, and on the basis of both this observation and the alcohol uptake values in Table 1, we propose that a maximum of two ethanol molecules may be present at the vicinity of a Brønsted acid site.

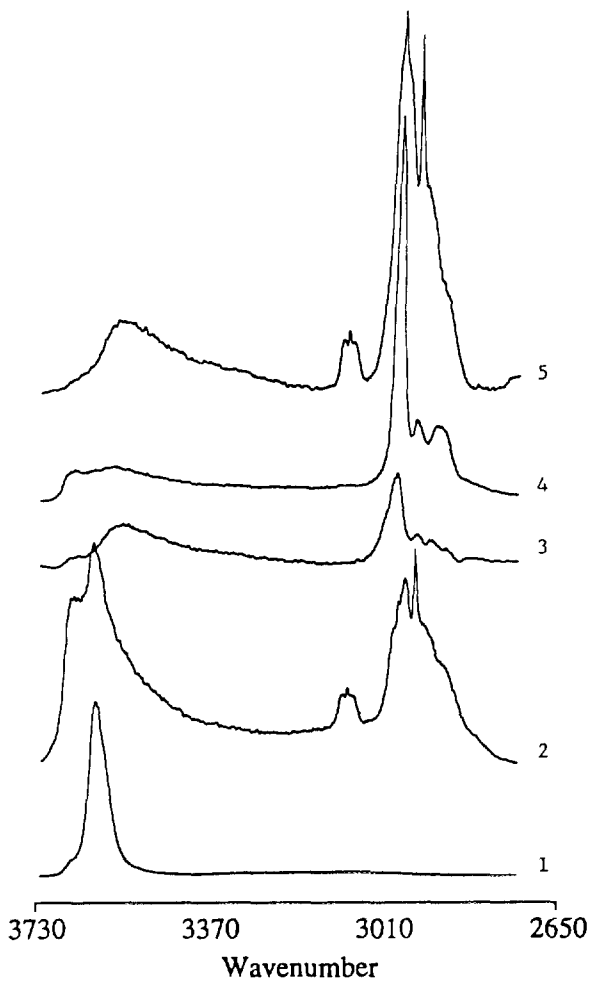

FIG. 7. The DRIFTS spectra in the 3700–2700 cm^{-1} region of (1) dehydrated H-mordenite, and after a 0.5 h steady flow of a 51 cc/min blend of nitrogen with (2) isobutene (P_{isob} = 0.7 kPa), (3) ethanol ($P_{ethanol}$ = 0.3 kPa), (4) ETBE (P_{ETBE} = 4.0 kPa), and (5) ethanol + isobutene (partial pressures of 0.3 and 0.7 kPa, respectively). Full scale: 0.83 Kubelka–Munk units..

Figure 7 shows that during isobutene/ethanol cofeeding experiments the O–H IR region resembles that observed during the pure ethanol feed run. The small band around 3100 cm^{-1} is attributed to $\nu(CH_2)$ (vinyl protons). There is an increase in the C–H stretching region consistent with the presence of isobutene in the zeolite channels, but note that the influence of isobutene on the O–H region when admitted in the DRIFTS cell alone differs from that of the (isobutene + ethanol) reacting mixture. This suggests that ethanol may act as a poison for the direct interaction of the olefin double bond with the acid sites and as a consequence, for the olefin oligomerization pathway. It is not obvious why the isobutene C–H stretching intensity is higher during ethanol cofeeding. One possibility is that, in the absence of ethanol, poisoning occurs rapidly at the pore mouth of the zeolite preventing further diffusion of isobutene into the mordenite channels. We expect the oligomerization of an olefin with a doubly substituted C=C bond on an alcohol-free zeolite to be an extremely fast reaction (21). It has to be understood that this argument implies that the characteristic reaction times are much shorter than the diffusion times since the gaseous isobutene molecules would not be free to travel through the pores significantly before they react. The transition from a π-coordinated olefin to the protonated form has been detected by Spoto *et al.* (20). These authors found that, upon loading of H-ZSM5 catalysts with propene at room temperature, a short-lived (approximately 5–10 s) broad band around 3200 cm^{-1} is formed accompanied by the disappearance of the zeolite O–H stretching band. When using ethene instead, the π-coordinated–protonated olefin transition occurred at rates slow enough to allow the oligomerization process to be studied in more detail (21). We have been unable to observe the formation of a similar band during transient studies with isobutene at 337 K, presumably due to the extremely short life of the π-coordinated species.

During reaction, the whole C–H stretching region is expected to be a convolution of bands resulting from reactants, product adsorption, and zeolite O–H stretching. It is not evident from Fig. 7 whether adsorbed ETBE was essentially absent during reaction. On the other hand, under continuous ETBE feeding of the DRIFTS chamber, the C–H stretching region is dominated by a strong $\nu(CH_3)$ band consistent with the large methyl proton density of the product molecule. Judging from the O–H region, the ether also appears to interact with the zeolite acid sites.

The 1750–700 cm^{-1} region of the spectra under steady flow conditions is shown in Fig. 8. Note that strong zeolite lattice deformation bands are present, and that ethanol (and ETBE) causes the band at 1350 cm^{-1} to shift to lower frequencies. This could be taken as an additional indication of strong interaction between the zeolite framework and the polar species. We would have preferred to present the data in this region as difference spectra but this shift did not make the small new features more clear. During reaction and with isobutene alone, the spectrum shows an increase in the band around 1640 cm^{-1}, which can be assigned to ν(CC). The gas-phase C–C stretching frequency is 1623 and 1647 cm^{-1} for ethylene and propylene, respectively, and they experience downward shifts on the order of 10–30 cm^{-1} before oligomerization starts taking place (21). For MTBE, a strong band at 1091 cm^{-1} is assigned to ν_{asym}(C–O) and the 1209 cm^{-1} signal is believed to be due to an antisymmetric C–O–C angle deformation involving the *tert*-butyl group (22). Figure 8 shows that ETBE filling of the H-mordenite pores results in the appearance of similar strong bands at 1070 and 1190 cm^{-1}. The small sharp signal at 890 cm^{-1} observed in the presence of isobutene is a typical strong absorption feature of alkenes due to out-of-plane C–H deformation vibrations. Thus, this band is likely to result from the small amount of gas-phase isobutene in the cell. Figure 8 also shows that adsorbed ETBE or ethanol cause the appearance of 1360–1390 and 1450 cm^{-1} bands that can be assigned to saturated C–H deformations. The 1360–1390 cm^{-1} C–H deformation band may also be convoluted with the strong zeolite lattice deformation band in the case of spectrum 2 in Fig. 8. For the sake of brevity and given the fact that the zeolite displays poor reflectivity at low frequencies, we will discuss our *in situ* experiments mostly in terms of changes induced in the high frequency end of the DRIFTS spectra by changes in feed composition. This will not affect the conclusion presented below.

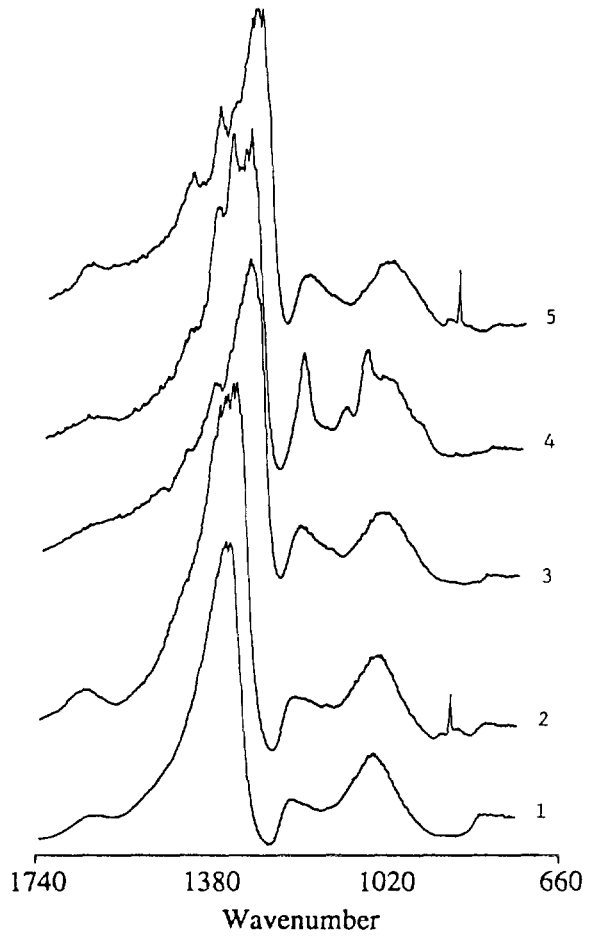

FIG. 8. DRIFTS spectra in the 1750–700 cm^{-1} region. Labels correspond to those of Fig. 7. Full scale: 8.4 KM units.

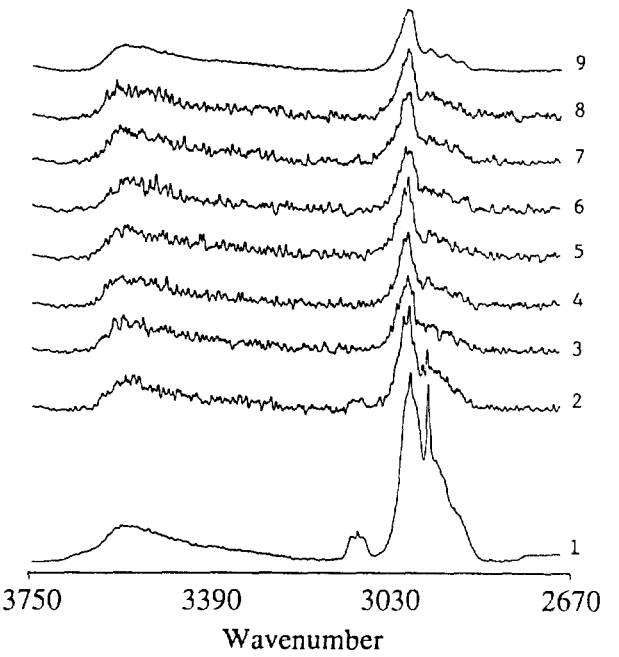

FIG. 9. DRIFTS spectra after replacing the isobutene flow with nitrogen. (1) Steady state (t = 0 min), (2) 0.5 min, (3) 1.5 min, (4) 2.5 min, (5) 3.5 min, (6) 4.5 min, (7) 5.5 min, (8) 6.5 min, (9) 50 min. Full scale: 0.83 KM units. The partial pressure of reactants prior to flow-switching is the same as in Fig. 7.

Figure 9 shows the effect of replacing the isobutene flow with nitrogen on the 2700–3700 cm^{-1} range while keeping the alcohol flow constant. The lower quality of the data at short times is due to a decrease in the data acquisition time by a factor of 0.05. It is noticed that isobutene is removed after a few seconds from the pores when alcohol is present, and the spectrum after purging of the olefin is very similar to that of the alcohol-loaded zeolite (see Fig. 7). The low-frequency side of spectra 1 and 9 in Fig. 9 is displayed in Fig. 10, where the complete disappearance of the 890 and 1640 cm^{-1} signals due to isobutene is noticed. Figure 11 shows the effect of replacing various feeds with nitrogen on the high-frequency end of the DRIFTS spectra, after long purging times (0.5 h). Prior to flow switching, the catalyst bed was allowed to react with the chosen gas composition for 0.5 h. Remarkably, desorption of ETBE gives a very similar spectrum to that resulting from desorption of a pure ethanol feed. This implies that ETBE decomposed over H-mordenite (to a small extent) prior to desorption. Another interesting feature is the appearance of a high-frequency shoulder in the O–H band in all cases in which ethanol (or pure ETBE) was desorbed. This would suggest that it is only after long nitrogen purging times that the alcohol–H· interaction observed at low alcohol coverages is partially recovered. We propose that single ethanol molecules adsorbed on the acid sites give rise to the higher frequency O–H band. We do not believe that this shoulder was due to the interaction of isobutene (as product of ETBE decomposition) with the acid sites since

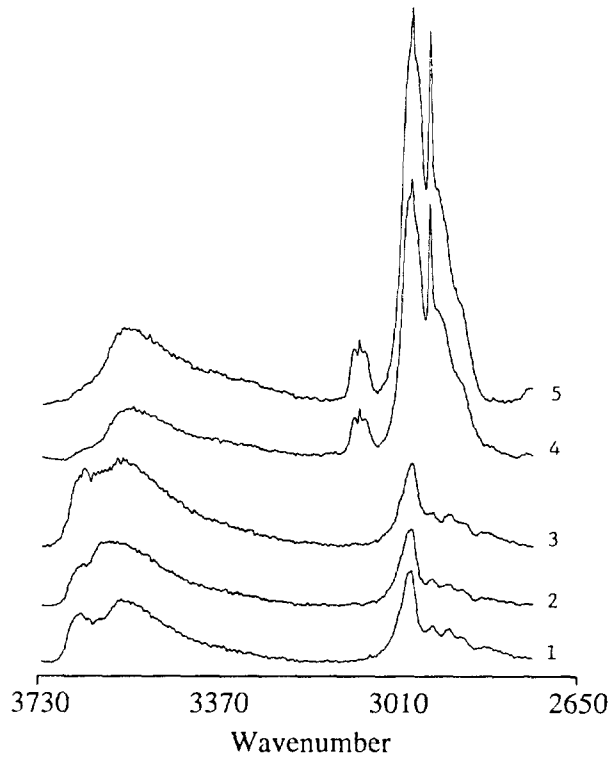

FIG. 11. DRIFTS spectra after 0.5 h since the following reactor feeds had been replaced by pure nitrogen. (1) ETBE, (2) ethanol, (3) isobutene + ethanol, (4) ethanol only, from an isobutene + ethanol feed. Spectrum (5) is for the isobutene + ethanol feed under the steady state. Full scale: 0.83 KM units. Partial pressures prior to desorption shown in Fig. 7.

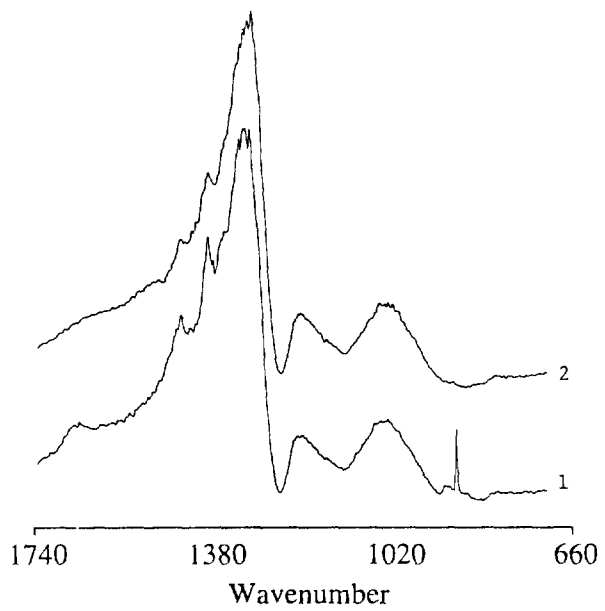

FIG. 10. Spectra in the 1750–700 cm^{-1} region under (1) steady-state (ethanol + isobutene) feed and (2) 50 min after replacing the isobutene flow with nitrogen. Full scale: 8.5 KM units.

no isobutene or heavier hydrocarbon bands were detected in the DRIFTS spectrum. From Fig. 11, the desorption of ethanol while a constant isobutene feed is maintained gives a spectra similar to that of the system under steady flow. If a continuous isobutene flow is kept and if single hydrogen-bonded alcohol molecules were in fact the electrophilic agents, one would expect the concentration of the latter to be small due to reaction. Note that the high-frequency contribution to the O–H stretching band after desorption of the reversible alcohol fraction, which we propose to be due to single hydrogen-bonded ethanol molecules, is smallest when the isobutene flow is maintained. Figure 11 also shows that after removal of both gas-phase ethanol and isobutene the resulting spectrum is also consistent with this picture since there is a stronger contribution of high-frequency O–H vibrations to the DRIFTS spectrum. A markedly different situation is apparent when a pure isobutene feed is desorbed (see Fig. 12 and compare with Fig. 7, spectrum 2). Spoto *et al.* (21) showed that a broad band in the 3300–3650 cm^{-1} range results from interaction of acidic –OH groups and saturated oligomeric chains. The

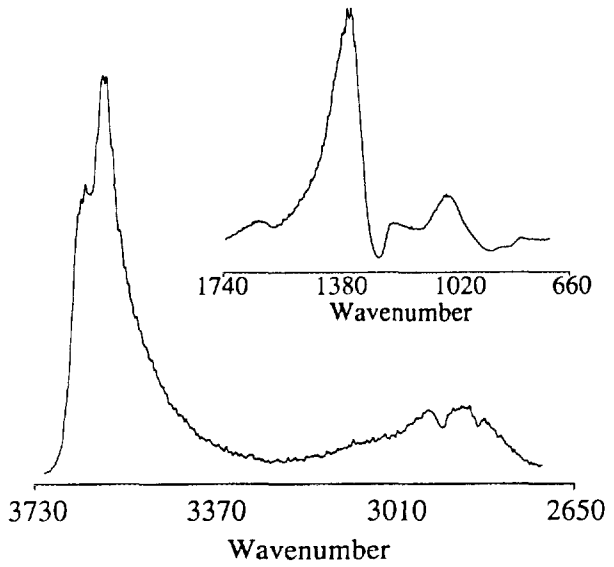

FIG. 12. DRIFTS spectra after 0.5 h since the isobutene flow (no ethanol present) had been replaced by nitrogen. The inset of the figure is for the low-frequency region. Full scale: 0.32 KM units. Inset: 8.4 KM units. Isobutene partial pressure prior to flow-switching: 0.7 kPa.

fact that a broad band (3350–3700 cm^{-1}) forms when only allowing isobutene in the cell and that some −OH groups remain unperturbed is consistent with both the arguments presented in Ref. (21) and the idea that pore blockage occurs rapidly in the absence of ethanol. We do not expect the appearance of this broad band overlapping the O–H signal to be due to perturbation of the latter by olefin double bonds because, as mentioned earlier, the lifetime of a π-coordinated isobutene–H^+ complex at 337 K is expected to be extremely short. A small broad band in the C–H stretching region is also evident in Fig. 12, suggesting that some hydrocarbon species cannot be removed by nitrogen purging. We can offer no explanation at this time as to why, upon perturbation of the steady state by interruption of the ethanol flow, we observe a decrease in the IR bands associated with isobutene since on the basis of Fig. 3, the opposite trend was expected. The ν(CC) band (inset Fig. 12) suggests that olefinic bonds were still present in the catalyst after purging of the excess isobutene.

The DRIFTS spectra under different conditions and the kinetic results suggest that (i) the interaction of ethanol with the H–mordenite acid sites depends on the extent of pore filling. When ethanol is allowed in the zeolite pores at ethanol/H^+ ratios below 1 hydrogen-bonded species start to appear but the O–H stretching signal shifts to lower frequencies (weaker O–H bonds) only when excess alcohol is present. Another salient feature is that after the zeolite was saturated with ethanol, only a small fraction of ethanol desorbed at the reaction temperature. The remaining ethanol/H^+ ratio upon desorption still exceeded the value of 1 even when gas-phase isobutene was present. The features observed in the O–H stretching region at low ethanol coverages are never fully restored by desorption of the reversible ethanol fraction. This is consistent with the idea that low molecular weight alcohols have a tendency to form rather stable clusters in zeolites. (ii) In the presence of ethanol, isobutene does not interact significantly with the acid sites (or at least it does not interact in the same way when alcohol is absent), a fact that may be crucial to prevent olefin oligomerization and catalyst deactivation. (iii) ETBE decomposes, to a small extent, over H–mordenite leaving behind chemisorbed alcohol molecules, and does not accumulate significantly under the reaction conditions employed here. (iv) The inhibitor character of ethanol may be due to the formation of an alcohol-crowded acid site that would adversely affect the electrophilic attack of the olefin on the basis of both steric arguments and the formation of weaker electrophilic species. A reaction scheme in which ETBE formation proceeds via protonation of the olefin first would also be affected by a strong affinity of Brønsted acid sites for alcohol molecules. However, if this were the case we would still expect the presence of measurable amounts of isobutene under the steady state in the zeolite pores to yield, to some extent, oligomerization products and catalyst deactivation given the extremely

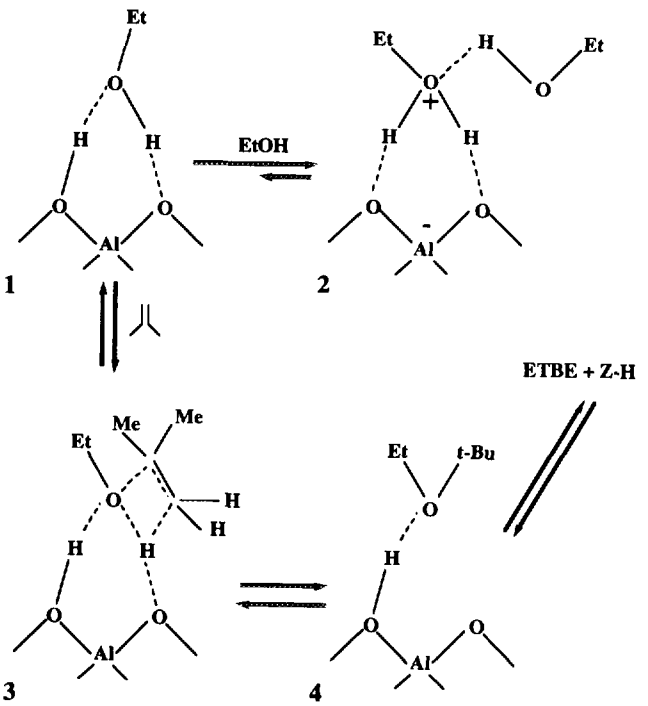

FIG. 13. Proposed reaction scheme.

fast nature of this reaction pathway. We have noticed that after a full day on stream the activity of H–mordenite toward ETBE formation remains unchanged. Thus, we propose that the alcohol plays a key role in both catalyst stability and reaction inhibition, and that the isobutene double bond is likely to be attacked by a single hydrogen-bonded ethanol molecule.

A tentative reaction scheme is shown in Fig. 13. The reaction pathways leading to ETBE are expected to be reversible under the temperature and pressure ranges used in our study (8). Indeed, Fig. 11 shows that after feeding the DRIFTS reactor cell with pure ETBE followed by nitrogen purging the spectrum essentially resembles that of adsorbed ethanol. *A priori*, at least two structures can be proposed for the interaction of the zeolite acid site with the ethanol molecule. Based on *ab initio* calculations, the so-called ion-pair (IP) structure which implies charge separation (methoxonium ion) has been proposed as a transition state for the hydrogen exchange reaction between the zeolite and the alcohol, rather than a minimum in the potential energy surface (PES) (23, 24). On the other hand, the cyclic, hydrogen-bonded structure 1 in Fig. 13 was found to be an absolute minimum in the PES (23). Van Santen and Kramer (25) have also indicated that the hydrogen-bonded structure provides a more accurate explanation of the IR spectra of moderate bases such as alcohols. Based on an extensive literature search, the work of Haase and Sauer (20) appears to provide the only theoretical support for structure 2. These authors pointed out that such IP species may exist at high alcohol loadings, since the predicted ^{1}H NMR shifts agree well with experimental data on the methanol/H-ZSM-5 system (19). However, it appears that theoretical studies dealing with clusters of at least two alcohol molecules interacting with the zeolite acid sites are still in demand. Note that one may intuitively favor an open chain hydrogen-bonded structure given the well-known tendency of such bonds to occur on a single plane. Structure 3 is tentatively proposed but has yet no theoretical support. Note that this particular step provides an interesting opportunity for the study of the reaction with isotopic labeling of the zeolite or the reactant molecules. Theoretical studies are currently under way in our laboratory to determine the energetics of the zeolite–ether interaction (structure 4) and to evaluate the stability of such adduct.

There is both theoretical (26) and experimental (21) evidence to support a mechanism of olefin oligomerization that proceeds via π-bonding of the olefin with the acid site first, followed by "alkoxylation" of the zeolite. Using *in situ* ^{13}C NMR, Haw *et al.* (27) found that alkoxy species are long-lived reactive intermediates in the polymerization of propene over HY zeolite. Figure 4 shows that a small amount of oligomeric species is able to leave the zeolite pores but the time on stream profiles suggest that catalyst deactivation by pore plugging occurs rapidly in the absence of ethanol.

4. CONCLUSIONS

Under differential conversion regimes, the gas-phase reaction of ethanol with isobutene over H–mordenite results in the exclusive formation of ETBE. Ethanol is preferentially adsorbed on the acid sites but its high concentration in the H–mordenite pores found during reaction is likely to be due to molecular clustering. The same high affinity of zeolite protons for alcohol molecules also appears to be responsible for both catalyst stability and the inhibitory effect of ethanol.

ACKNOWLEDGMENTS

This research was supported in part by the National Science Foundation, Division of Chemical and Transport Systems (Grant CTS-940618), the EPSCoR National Science Foundation Program (Grant OCR-9255225), and the Center for Materials Research and Analysis at the University of Nebraska-Lincoln. Two of us, H.S.S. and E.L., wish to express their appreciation to the University of San Juan (Argentina) and COLCIENCIAS (Colombia), respectively, as recipients of visiting scholarship awards. We also thank the reviewers for their valuable comments.

REFERENCES

1. Piel, W. J., and Thomas, R. X., *Hydrocarbon Process.* 68 (1990).
2. Fité, C., Iborra, M., Tejero, J., Izquierdo, J. F., and Cunill, F., *Ind. Eng. Chem. Res.* **33,** 581 (1994).
3. Kogelbauer, A., Ocal, M., Kikolopoulos, A. A., Goodwin Jr., J. G., and Marcelin, J., *J. Catal.* **148,** 157 (1994).
4. Vila, M., Cunill, F., Izquierdo, J. F., González, J., and Fernández, A., *Appl. Catal. A: General* **117,** L99 (1994).
5. Izquierdo, J. F., Vila, M., Tejero, J., Cunill, F., and Iborra, M., *Appl. Catal. A: General* **106,** 155 (1993).
6. Tejero, J., Cunill, F., and Iborra, M., *J. Mol. Catal.* **42,** 257 (1987).
7. Nikolopoulos, A., Palucka, T. P., Shertukde, T. P., Oukaci, R., Goodwin Jr., J. G. and Marcelin, G., "Proceedings, 10th International Congress on Catalysis, Budapest, July 1992." (L. Guczi *et al.*, Eds.), p. 2601. Akadémiai Kiadó, Budapest, 1993.
8. Le Vanmao, R., Alhafi, H., and Le, T. S., *in* "Selectivity in Catalysis" (M. E. Davis and S. L. Suib, Eds.), ACS Symposium Series 517, Chap. 16. Am. Chem. Soc., Washington, DC, 1993.
9. Tau, L-M., and Davis, B. H., *Appl. Catal.* **53,** 263 (1989).
10. Lewis, R. B., *Nat. Resour. Tax Rev.* 1079, 1994.
11. Ancillotti, F., Mauri, M. M., and Pescarollo, E., *J. Catal.* **46,** 49 (1977).
12. Bell, A. T., Manzer, L. E., Chen, N. Y., Weekman, V. W., Hedegus, L. L., and Pereira, C. J., *Chem. Eng. Progr.* **91,** 26 (1995).
13. Thornton, R., and Gates, B. C., *J. Catal.* **34,** 275 (1974).
14. Xiao, J., and Wei, J., *Chem. Eng. Sci.* **47,** 1143 (1992).
15. Makarova, M. A., Paukshtis, E. A., Thomas, J. M., Williams, C., and Zamaraev, K. I., *J. Catal.* **149,** 36 (1994).
16. Kogelbauer, A., Nikopoulos, A. A., Goodwin Jr., J. G., and Marcelin, G., *J. Catal.* **152,** 122 (1995).
17. Chen, N. Y., Degnan Jr., T. F., and Smith, C. M., "Molecular Transport and Reaction in Zeolites: Design and Application of Shape Selective Catalysts" Chap. 4. VCH, Weinheim/New York, 1994.

18. Breck, D. W., "Zeolite Molecular Sieves: Structure, Chemistry and Use." Wiley, New York, 1974.
19. Mirth, G., Lercher, J. A., Anderson, M. W., and Klinowsky, J., *J. Chem. Soc. Faraday Trans.* **86,** 3039 (1990).
20. Haase, F., and Sauer, J., *J. Phys. Chem.* **98,** 3083 (1994).
21. Spoto, G., Bordiga, S., Ricchiardi, G., Scarano, D., Zecchina, A., and Borello, E., *J. Chem. Soc. Faraday Trans.* **90,** 2827 (1994).
22. Nyquist, R. A., "The Interpretation of Vapor-Phase Infrared Spectra: Group Frequency Data." Sadtler Research Labs Press, 1984.
23. Haase, F., and Sauer, J., *J. Am. Chem. Soc.* **117,** 3780 (1995).
24. Blaszkowski, S. R., and van Santen, R. A., *J. Phys. Chem.* **99,** 11728 (1995).
25. van Santen, R. A., and Kramer, G. J., *Chem. Rev.* **95,** 637 (1995).
26. Kazansky, V. B., and Senchenya, I. N., *J. Catal.* **119,** 108 (1989).
27. Haw, J. F., Richardson, B. R., Oshiro, I. S., Lazo, N. D., and Speed, J. A., *J. Am. Chem. Soc.* **111,** 2052 (1989).